



Missouri University of Science and Technology
Scholars' Mine

International Specialty Conference on Cold-Formed Steel Structures

(1971) - 1st International Specialty Conference on Cold-Formed Steel Structures

Aug 20th, 12:00 AM

Strength and Stiffness of Steel Deck Shear Diaphragms

Duane S. Ellifritt

Larry D. Luttrell

Follow this and additional works at: <https://scholarsmine.mst.edu/isccss>

 Part of the [Structural Engineering Commons](#)

Recommended Citation

Ellifritt, Duane S. and Luttrell, Larry D., "Strength and Stiffness of Steel Deck Shear Diaphragms" (1971). *International Specialty Conference on Cold-Formed Steel Structures*. 1. <https://scholarsmine.mst.edu/isccss/1iccfss/1iccfss-session4/1>

This Article - Conference proceedings is brought to you for free and open access by Scholars' Mine. It has been accepted for inclusion in International Specialty Conference on Cold-Formed Steel Structures by an authorized administrator of Scholars' Mine. This work is protected by U. S. Copyright Law. Unauthorized use including reproduction for redistribution requires the permission of the copyright holder. For more information, please contact scholarsmine@mst.edu.

STRENGTH AND STIFFNESS OF STEEL

DECK SHEAR DIAPHRAGMS

By

Duane S. Ellifritt¹

and

Larry D. Luttrell²

In conventional steel construction, floor and roof joists are often overlaid with a light gage steel sheet which has been roll-formed into a trapezoidally corrugated shape and commonly referred to as "steel deck." It is usually formed into 18, 24, 30, or 36 inch panels and serves the primary function of transmitting live, dead, and construction loads into the structure. To do this efficiently, a great variety of deck configurations have been developed.

When steel deck is welded to a structural steel framework, it forms a shear-resistant panel known as a "shear diaphragm," which may be used to resist in-plane forces arising from wind or earthquake, in addition to the usual gravity loading. The ability to transmit in-plane loads to the framework is dependent on two parameters, viz., stiffness and ultimate strength. A general solution for these is complicated by the wide range of deck configurations, methods of fastening, and condition of installation. This paper reports the results of research on three general types of steel deck under various conditions of fastener arrangement, purlin spacing, gage, and material yield strength.

In the investigation reported herein, the three types of deck tested were: narrow rib, known in the trade as "A" deck, wide rib, or "B" deck, and intermediate rib deck. Typical cross sections of the three types are shown in Figure 1. Among the wide rib decks tested, there were two variations in the side lap arrangement. The standing seam side lap was given the designation "WB" to distinguish it from the more conventional flat side lap, designated "W." Both types are shown in Figure 2.

Tested diaphragms were evaluated with respect to the two major behavioral parameters, ultimate strength and shear stiffness. The former is given the symbol S_u and designates the total jacking force required to produce failure in a diaphragm divided by the length of the diaphragm in the direction of the applied load. Shear stiffness, G' , is a measure of the relationship between in-plane load and the deflection in the direction of that load. Units are kips per inch of deflection and calculation follows the secant modulus recommendation in the American Iron and Steel Institute Bulletin, "Design of Light Gage Steel Diaphragms (1), as shown in Figure 3.

EXPERIMENTAL PROGRAM

Tests were made on 16, 18, 20, and 22 gage decks with lengths of 12, 16, and 20 feet. Panel widths tested were 18, 24, 30, and 36 inches. The test program was designed to account for the effects of panel configuration, purlin spacing, sheet thickness, material yield strength, and the arrangement of fasteners. All tests were made on a horizontal cantilever test frame according to the procedure outlined in the American Iron and Steel Institute Bulletin (1). The connections between the perimeter members of the frame were made with light clip angles and considered as pinned. The entire frame was supported on rollers to eliminate the possibility of developing frictional resistance during deformation. Pur-

¹Assistant Professor, Oklahoma State University, Stillwater, Oklahoma.

²Associate Professor, West Virginia University, Morgantown, West Virginia.

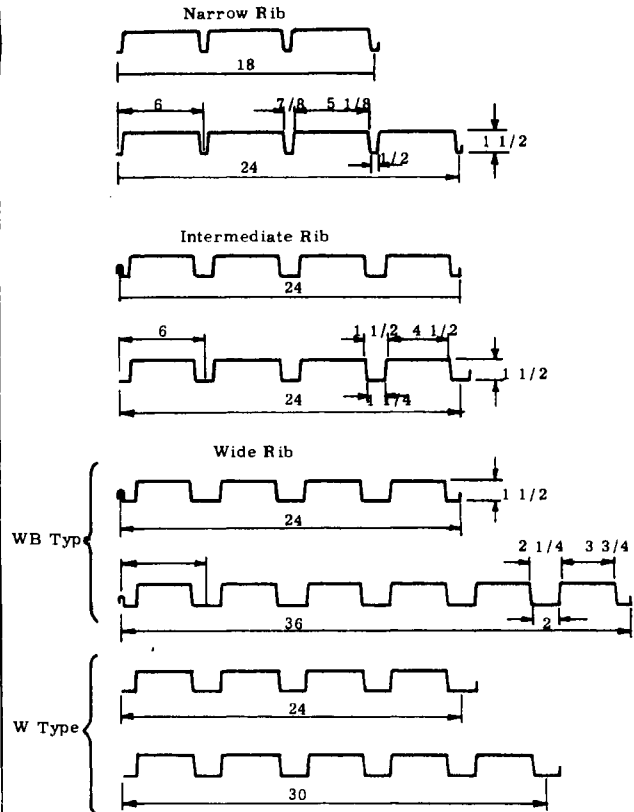
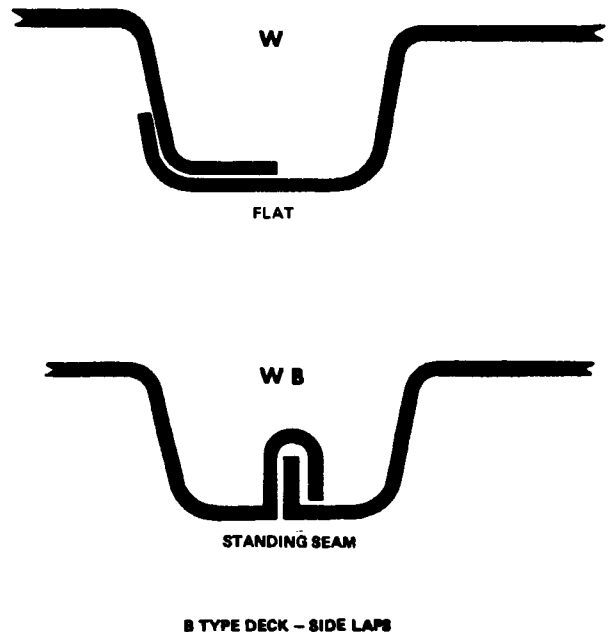
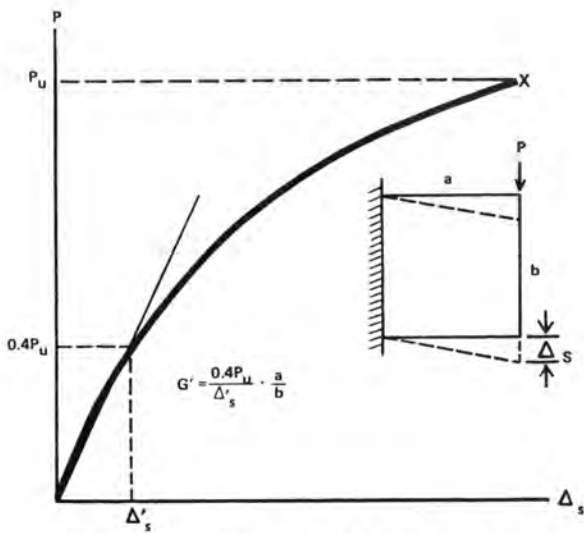


Fig. 1. Types of Deck Tested



B TYPE DECK - SIDE LAPS

Fig. 2. Types of Side Laps



Calculation of Diaphragm Stiffness - AISI Method

Fig. 3. Method of Calculating Diaphragm Stiffness from Test
 lins were fastened to the frame with pinned connections and spacing was variable. An illustration of the test frame is shown in Figure 4.

Welds were made with E6013 1/8" diameter electrodes with sufficient heat for fusion. Various weld arrangements were used; the most common being a weld in every other valley and hereafter referred to as the "standard" case. Some diaphragms had extra welds on the ends of the sheets and others were fastened along side laps between purlins. Other fastener patterns used are shown in Figure 5. The key to the weld designation shown in Table 1 appears in Figure 6. It should be noted that the standing seam sidelaps (WB type) were welded on both sides of the seam.

The loading apparatus for all tests consisted of one hydraulic jack and load cell arrangement in line with the center line of the south edge member at the southwest corner as shown in Figure 7. A tensile load was applied by means of a high strength rod threaded through the reaction frame and connected to the edge beam at a level where the diaphragm attaches to the frame. Load was applied in increments from zero to failure with deflection measurements made at each stage of loading. Deflections were measured with Ames dial gages accurate to 0.001" at all corners in the plane of the diaphragm as shown in Figure 8. From these measurements it was possible to correct for support movement and arrive at the true diaphragm deflection Δ , according to the formula,

$$\Delta = \Delta_4 - (\Delta_2 + \frac{a}{b} (\Delta_1 + \Delta_5))$$

where Δ_1 , Δ_2 , Δ_4 , and Δ_5 are measured movements at the corners in inches



Fig. 4. The Test Frame

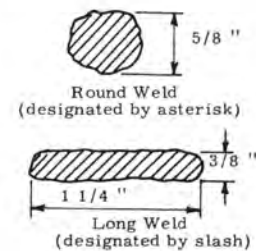
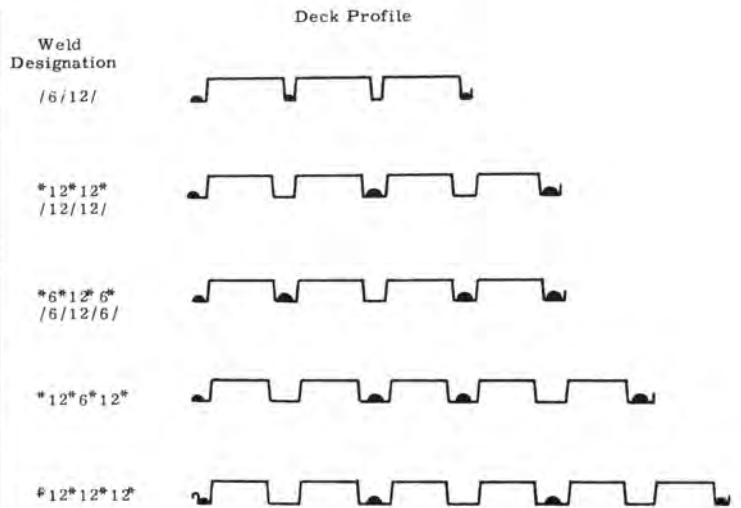
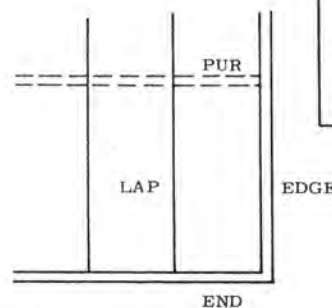


Fig. 5. Various Weld Patterns Used in Tests

Fastener Locations



Symbols

*	5/8" diameter round weld
/	3/8 x 1 1/4" long weld
)	Button punch on sidelap
:	Seam weld, sidelap

Sample Designation

Description

END	/12*12/	The ends of the sheet are welded to the perimeter member in a repeating pattern of alternating long and round welds 12" o. c.
PUR	*12*12*	The sheet is welded to each purlin with round welds 12" o. c.
LAP)30(.	Sidelaps are button-punched on 30" centers
EDGE	*24*	Longitudinal edge of sheet is welded to perimeter member on 24" centers
LAP	:20:	Bead welds spaced at 20" on sidelaps

Fig. 6. Key to Weld Designations

a = diaphragm dimension perpendicular to the loading direction
 b = diaphragm dimension parallel to the loading direction

Three standard tensile coupons were taken randomly from each shipment of material and tested. All paint or galvanized coating was removed prior to thickness measurement and testing.

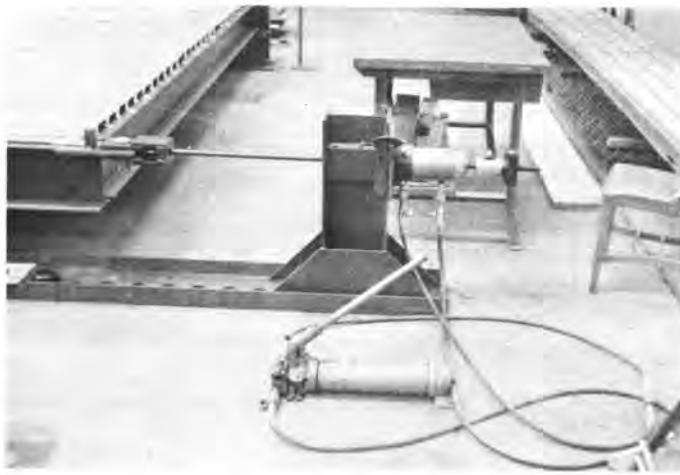


Fig. 7. Load Frame and Jack

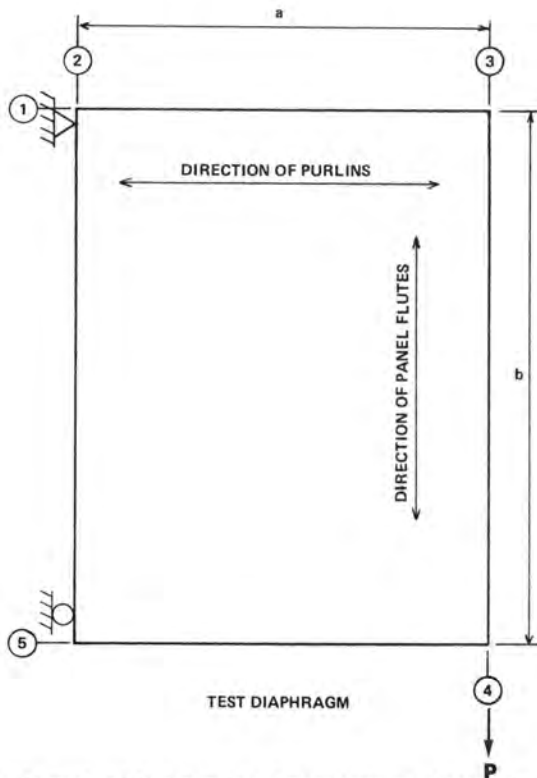


Fig. 8. Schematic of Diaphragm Test Showing Location of Deflection Gages

TEST RESULTS

Test results are tabulated in Table 1. In each test, the diaphragm was loaded to failure, which was initiated in a variety of ways. If a weld failed, it was generally because of the sheet tearing away from the weld. This was always accompanied by large in-plane displacements before the sheet separated entirely, and this in turn increased the likelihood of rib buckling. A good illustration of sheet tearing at the welds can be seen in Figures 9 and 10. Although unusual, welds sometimes separated cleanly from the perimeter beam while still attached to the sheet, as shown in Figure 11. This phenomenon usually occurred at a sheet side lap where the weld was made through two thicknesses of material and there was insufficient weld heat to produce adequate penetration into the perimeter member. This type of weld failure was sudden and was not preceded by large displacements as was the sheet tearing-type failure.

Before discussing the buckling-type failure, some qualification or

the word "buckling" is necessary. If the edge flute of a panel is thought of as a hat-shaped column as shown in Figure 12, it can be seen that the "column" receives loads from in-plane shear forces in the diaphragm. It is loaded eccentrically with respect to both centroidal axes and, unlike common buckling problems, the flute begins to bend upward and twist as soon as the first load is applied. As deflections become large, the

Table 1(a). Test Summary, "B" Deck, W-Series Tests

Test Number	Fastener Pattern				Purlin Spacing (ft)	Sheet Thickness (in)	G' (k/in)	S _u (plf)
	End	Pur	Lap	Edge				
W-24-20-20-1	/12*12/	/12*12/	None	None	4'-0	.0348	15.2	624
W-24-20-20-2	"	"	"	"	5'-0	.0355	18.4	605
W-24-22-20-3	"	"	"	"	6'-8	.0288	10.6	320
W-24-20-20-4	"	"	"	"	4'-0	.0361	14.1	650
W-24-22-20-5	"	"	"	"	5'-0	.0288	11.1	401
W-24-22-20-6	"	"	"	"	4'-0	.0288	12.0	461
W-24-22-20-7	"	"	"	"	4'-0	.0305	16.2	508
W-24-20-16-8	"	"	"	"	5'-4	.0348	12.1	510
W-24-20-12-9	"	"	"	"	6'-0	.0348	9.4	467
W-30-18-20-10	/12/6/12/	/12/6/12/	"	"	5'-0	.0465	40.3	1040
W-30-20-20-11	"	"	"	"	5'-0	.0330	21.6	640
W-30-20-20-12	"	"	"	"	5'-0	.0360	20.7	630
W-30-20-20-13	/12*6*12/	"	"	"	5'-0	.0360	20.6	580
W-30-22-20-14	"	"	"	"	4'-0	.0290	15.9	560
W-30-22-20-15	/12/6/12/	"	"	"	5'-0	.0278	16.9	450
W-24-20-20-16	/6*12*6/	/12*12/	"	"	6'-8	.0348	23.2	505
W-24-22-20-17	"	"	"	"	6'-8	.0288	14.4	339
W-24-18-20-18	/12*12/	"	"	"	5'-0	.0465	21.3	830
W-24-20-20-19	"	"	:30:	"	5'-0	.0355	23.0	807
W-24-20-20-20	"	"	:20:	"	5'-0	.0355	24.9	912
* W-24-22-20-21	*12*12*	*12*12*	:24:	:24:	6'-8	.0280	6.8	375
* W-24-22-20-22	"	"	"	"	6'-8	.0280	9.1	417

* Screw-connected

Table 1(b). Test Summary, "B" Deck, WB-Series Tests

Test Number	Weld Pattern				Purlin Spacing (ft)	Sheet Thickness (in)	G' (k/in)	S _u (plf)
	End	Pur	Lap	Edge				
WB-24-18-20-1	*12*12*	*12*12*	None	None	5'-0	.0505	32.3	1260
WB-24-20-20-2	"	")20(:20:	6'-8	.0365	12.6	495
WB-24-20-20-3	"	"	None	None	6'-8	.0365	11.8	480
WB-24-20-20-4	"	"	"	"	4'-0	.0365	16.5	775
WB-24-20-20-5	"	"	"	"	5'-0	.0351	16.0	525
WB-24-20-20-6	"	"	"	"	5'-0	.0353	16.6	580
WB-24-22-20-7	"	"	"	"	6'-8	.0320	10.6	492
WB-24-22-20-8	"	"	"	"	4'-0	.0314	12.7	615
WB-24-22-20-9	"	"	"	"	4'-0	.0283	11.5	423
WB-24-22-20-10	"	"	"	"	6'-8	.0270	8.3	311
WB-24-22-20-11	"	"	"	"	6'-8	.0270	12.8	339
WB-24-16-16-12	"	"	"	"	5'-4	.0587	32.4	1577
WB-24-18-16-13	"	"	"	"	5'-4	.0496	19.4	1125
WB-24-20-16-14	"	"	"	"	5'-4	.0365	14.4	719
WB-24-20-16-15	"	"	"	"	5'-4	.0365	13.8	694
WB-24-20-12-16	"	"	"	"	6'-0	.0365	8.4	498
WB-24-20-20-17	*6*12*6*	"	"	"	6'-8	.0365	19.8	580
WB-24-20-16-18	"	"	"	"	5'-4	.0365	22.7	906
WB-36-18-20-19	*12*12*12*	*18*18*)20(:20:	5'-0	.0460	34.5	1400
WB-36-18-20-20	"	"	:20:	"	5'-0	.0460	32.0	1500
WB-36-20-20-21	"	")20("	5'-0	.0330	19.0	1025
WB-36-20-20-22	"	"	:20:	"	5'-0	.0330	19.0	950
WB-36-22-20-23	*12*12 12*	*18*18)20(:20:	5'-0	.0280	13.6	720
WB-36-22-20-24	"	"	:20:	"	5'-0	.0280	13.5	783
WB-36-18-16-25	"	")20("	8'-0	.0460	27.8	1140
WB-36-18-16-26	"	"	:20:	"	8'-0	.0460	26.3	1295
WB-36-20-16-27	"	")20("	8'-0	.0330	14.8	750
WB-36-20-16-28	"	"	:20:	"	8'-0	.0330	14.9	730
WB-36-22-16-29	"	")24(:24:	8'-0	.0280	10.1	540

* End Lapped

Table 1(b). Test Summary, "B" Deck, WB-Series Tests (continued)

Test Number	Weld Pattern				Purlin Spacing (ft)	Sheet Thickness (in)	G' (k/in)	S _u (plf)
	End	Pur	Lap	Edge				
WB-36-22-16-30	"	"	:24:	"	8'-0	.0280	8.3	530
WB-24-18-20-31	/12/12/	/12/12/	--	--	5'-0	.0455	27.4	1250
WB-24-22-20-32	"	"	"	"	5'-0	.0275	12.3	472
WB-24-18-20-33	/6/12/6/	"	"	"	5'-0	.0453	29.8	1400
WB-24-18-20-34	/12/12/	"	"	"	6'-8	.0455	23.0	1000
WB-24-18-20-35	"	"	"	"	4'-0	.0453	31.2	1400
WB-24-22-20-36	*6*12*6*	*12*12*	"	"	6'-8	.0320	15.4	348
WB-24-20-20-37	*12*12*	"	"	"	6'-8	.0365	12.8	409
WB-24-18-20-38	"	"	"	"	6'-8	.0496	17.6	460
WB-24-16-20-39	"	"	"	"	6'-8	.0587	31.0	738
WB-24-20-20-40	"	"	"	"	5'-0	.0365	13.1	696
WB-24-20-12-41	"	"	"	"	6'-0	.0365	10.2	583

Table 1(c). Test Summary, "A" Deck

Test Number	Weld Pattern				Purlin Spacing (ft)	Sheet Thickness (in)	G' (k/in)	S _u (plf)
	End	Pur	Lap	Edge				
A-24-22-20-1	/12/12/	/12/12/	None	None	5'-0	.0290	8.3	339
A-24-22-20-2	/12/12/	/12/12/	"	"	4'-0	.0290	10.1	432
A-24-22-20-3	/12/12/	/12/12/	"	"	6'-8	.0290	8.2	265
A-24-22-20-4	/6/12/6/	/12/12/	"	"	6'-8	.0290	11.7	240
A-24-20-20-5	/12/12/	/12/12/	"	"	6'-8	.0342	11.9	293
A-24-20-20-6	/6/12/6/	/12/12/	"	"	6'-8	.0342	13.3	396
A-24-18-20-7	/12/12/	/12/12/	"	"	6'-8	.0450	20.0	479
A-24-20-12-8	/12/12/	/12/12/	"	"	6'-0	.0342	7.8	411
A-24-22-20-9	/6/12/6/	/12/12/	"	"	6'-8	.0307	9.1	320
A-24-22-20-10	/6/12/6/	/12/12/	"	"	6'-8	.0307	9.4	316
A-24-20-20-11	/6/12/6/	/12/12/	"	"	6'-8	.0376	15.3	451
A-24-18-20-12	/6/12/6/	/12/12/	"	"	6'-8	.0497	26.1	706
A-24-18-20-13	/12/12/	/12/12/	"	"	6'-8	.0497	21.6	591
A-24-20-12-14	/12/12/	/12/12/	"	"	6'-0	.0376	6.6	408
A-18-18-20-15	/6/12/	/6/12/	"	"	6'-8	.0494	22.4	832
A-24-20-20-16	/12/12/	/12/12/	"	"	5'-0	.0348	12.6	565
A-18-22-20-17	/6/12/	/6/12/	"	"	6'-8	.0285	6.6	245
A-24-18-20-18	/12/12/	/12/12/	"	"	5'-0	.0448	20.9	820
A-18-22-20-19	/6/12/	/6/12/	"	"	5'-0	.0295	10.9	365
A-18-20-20-20	/6/12/	/6/12/	"	"	6'-8	.0350	13.0	548
A-24-20-20-21	/12/12/	/12/12/	"	"	4'-0	.0350	12.9	565
A-18-20-20-22	/6/12/	/6/12/	"	"	5'-0	.0355	14.1	507
A-18-18-20-23	/6/12/	/6/12/	"	"	5'-0	.0449	28.8	900
A-24-18-20-24	/12/12/	/12/12/	"	"	4'-0	.0444	26.5	750
A-24-20-20-25	/12/12/	/12/12/	"	"	10'-0	.0330	6.0	263
A-24-22-20-26	/12/12/	/12/12/	"	"	5'-0	.0296	9.3	425
A-24-22-20-27	/6/12/6/	/6/12/6/	"	"	5'-0	.0308	18.3	575
A-24-22-20-28	/6/12/6/	/12/12/	"	"	5'-0	.0272	11.6	365
A-24-18-20-29	/12/12/	/12/12/	"	"	5'-0	.0435	19.7	740

Table 1(c). Test Summary, "A" Deck (continued)

Test Number	Weld Pattern				Purlin Spacing (ft)	Sheet Thickness (in)	G' (k/in)	S _u (plf)
	End	Pur	Lap	Edge				
A-30-20-20-30	/12/6/12/	/12/6/12/	None	None	5'-0	.0337	15.7	550
A-30-22-20-31	"	"	"	"	6'-8	.0275	10.0	345
A-30-20-20-32	"	"	"	"	4'-0	.0337	20.1	615
A-30-22-20-33	"	"	"	"	5'-0	.0275	11.4	515

shape of the cross section changes (see Fig 13). The male rib tends to bend outward and the member rapidly loses stiffness. If the lip on the male rib is small, as in the narrow rib decks, sudden local buckling of the lip leads to overall buckling of the flute. In most cases, this takes place at a distance of about a flute width from a weld at the end of the panel, as shown in Figure 14. If the return on the male rib is large, as

Table 1(d). Test Summary, "I" Deck

Test Number	Weld Pattern				Purlin Spacing (ft)	Sheet Thickness (in)	G' (k/in)	S _u (plf)
	End	Pur	Lap	Edge				
I-24-20-20-1	*12*12*	*12*12*	None	None	10'-0	.0343	9.1	350
I-24-18-20-2	*12*12*	*12*12*	"	"	10'-0	.0469	17.5	550
I-24-18-20-3	*12*12*	*12*12*	"	"	6'-8	.0444	21.6	755
I-24-20-20-4	*12*12*	*12*12*	"	"	5'-0	.0345	16.1	535
I-24-22-20-5	*12*12*	*12*12*	"	"	5'-0	.0284	11.3	315
I-24-22-20-6	*12*12*	*12*12*	"	"	6'-8	.0284	8.0	275
I-24-20-20-7	*12*12*	*12*12*	"	"	6'-8	.0342	12.7	360
I-24-20-20-8	*6*12*6*	*12*12*	"	"	5'-0	.0342	24.8	520
I-24-22-20-9	*6*12*6*	*12*12*	"	"	6'-8	.0284	17.5	500
I-24-18-20-10	*6*12*6*	*12*12*	"	"	6'-8	.0477	36.6	750



Fig. 9. Tearing of Sheet Around Weld and Displacement



Fig. 10 Sheet Tearing and Displacement

in the wide rib decks, it acts as a stiffener to retard local buckling and the flute will generally fail as a slender compression strut. An illustration of this type of buckling is shown in Figure 15. In this report, buckling is taken to mean a sudden loss of lateral stiffness, but only after very large deflections and severe cross section distortion at the edge of the deck have developed.

In many of the diaphragms tested, weld failure and buckling were very closely allied and it was often difficult to assign precedence to one over the other. Generally, all the modes of failure were present to some degree. The loss of a side lap weld at a purlin suddenly increases the effective span and buckling of a flute may follow immediately. In

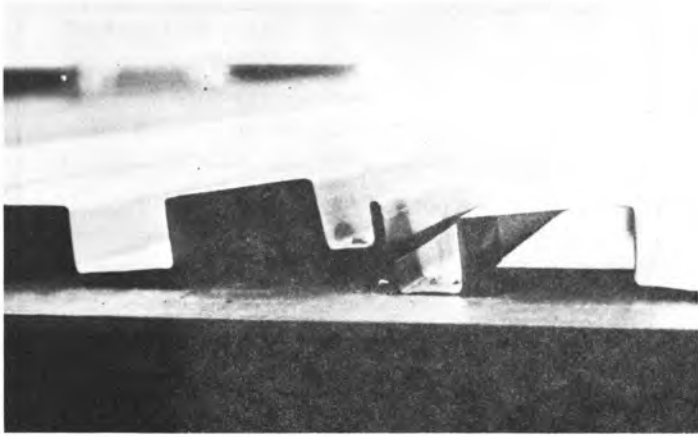


Fig. 11. Weld Failure by Separation from Frame

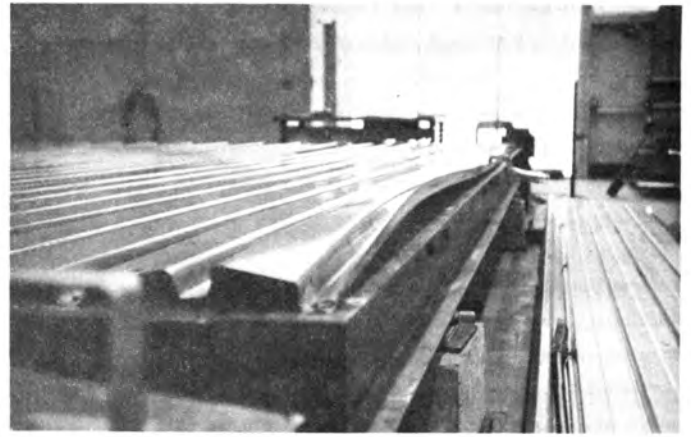


Fig. 13. Distortion of Panel During Buckling

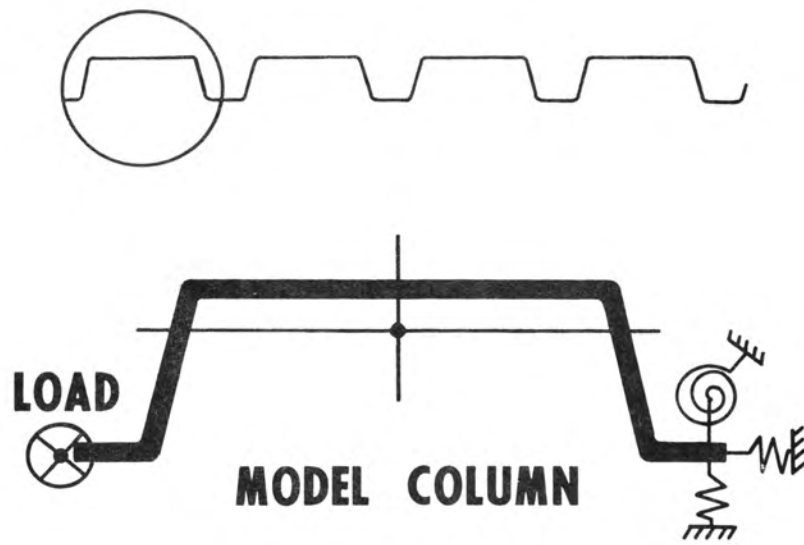


Fig. 12. Mathematical Model of Single Deck Flute

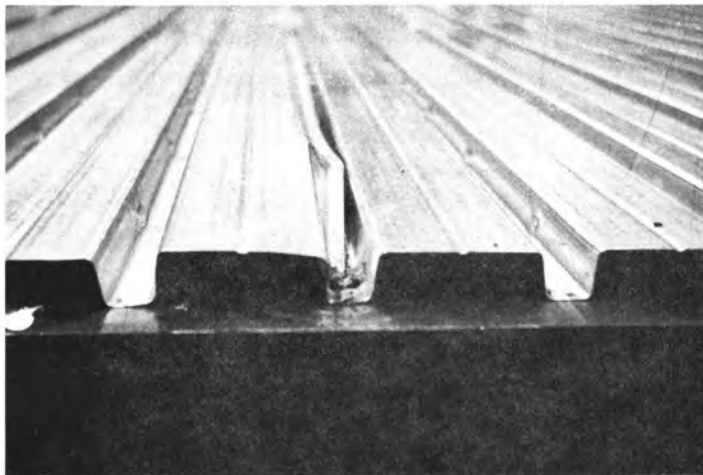


Fig. 14. Local Buckling of Male Rib of Edge Flute

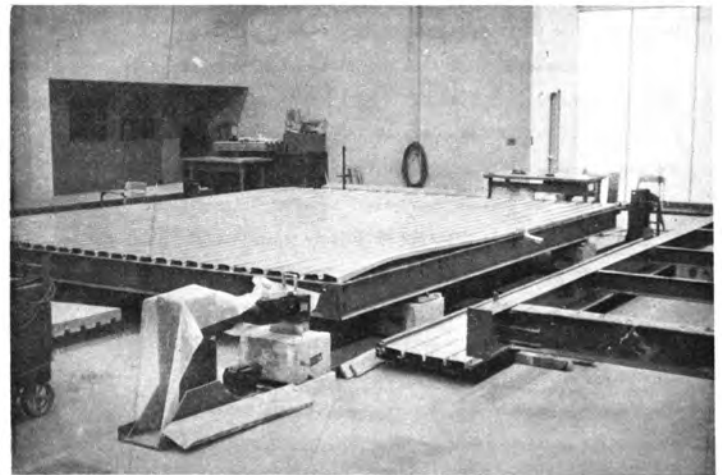


Fig. 15. Strut-like Buckling of Edge Flute

like manner, local buckling may cause a redistribution of load on the welds and may lead to sudden weld failures. It must be emphasized that the failure of a weld or the buckling of a flute did not necessarily mean that the ultimate diaphragm load had been reached. However, it was observed in tests that the additional increase in load after an initial failure of this type usually did not exceed ten percent.

ANALYSIS OF TEST RESULTS

Load-deflection curves were plotted from data taken during each diaphragm test. Those having similar characteristics were compared to determine the effect of changing one variable. Since most of the variables affecting diaphragm behavior are interrelated, it is not always possible to isolate the effect of a single variable. For example, the degree to which a change of gage influences stiffness may depend on the purlin spacing of the decks being compared. Similarly, the influence of an extra weld may not be the same for all panel widths. Thus, in the following section, comparisons of load-deflection curves are shown for those diaphragms which come closest to being identical, with respect to all variables except the one being investigated. Specific effects are studied in these cases and conservatively extrapolated to cover a broad range of decks not tested. Recommendations presented are representative average values for all diaphragms of a particular type.

The effects of single variables on diaphragm performance are summarized as follows:

Material Yield Strength. Normal fluctuations in yield strength associated with a particular grade of steel have insignificant effect on diaphragm behavior. An increase in yield strength tends to increase both strength and stiffness, but not linearly. In one case, shown in Figure 16, a 100% increase in yield strength boosted ultimate strength by 10% and stiffness by 35%. Reduced ductility in higher strength steels may be the cause of this non-linear behavior.

Panel Thickness. An increase in thickness causes strength and stiffness to be increased by an amount $\left(\frac{t_2}{t_1}\right)^\alpha$, where α varies

is nearly proportional to panel thickness when weld failure controls, but is related more closely to the square of the thickness when buckling controls. The low end of the range ($\alpha = 1.0$) represents local buckling failure and the upper end weld failure.

Panel Width. The influence of panel width is difficult to evaluate because it is so closely linked with weld spacing. Welds can only be made in the valleys between flutes. Since it is not common field practice to weld in every valley, this was not done in the tests. Thus, the number of welds per foot is different for each panel width. There is evidence, however, that wider panels make stronger and stiffer diaphragms because there are fewer side laps across which shear must be transferred, but the quantitative effect of panel width could not be determined from these tests.

Extra End Weld. Test results indicate that calculated strength and stiffness should be modified by coefficients Q and M, respectively, which are dependent on gage and deck

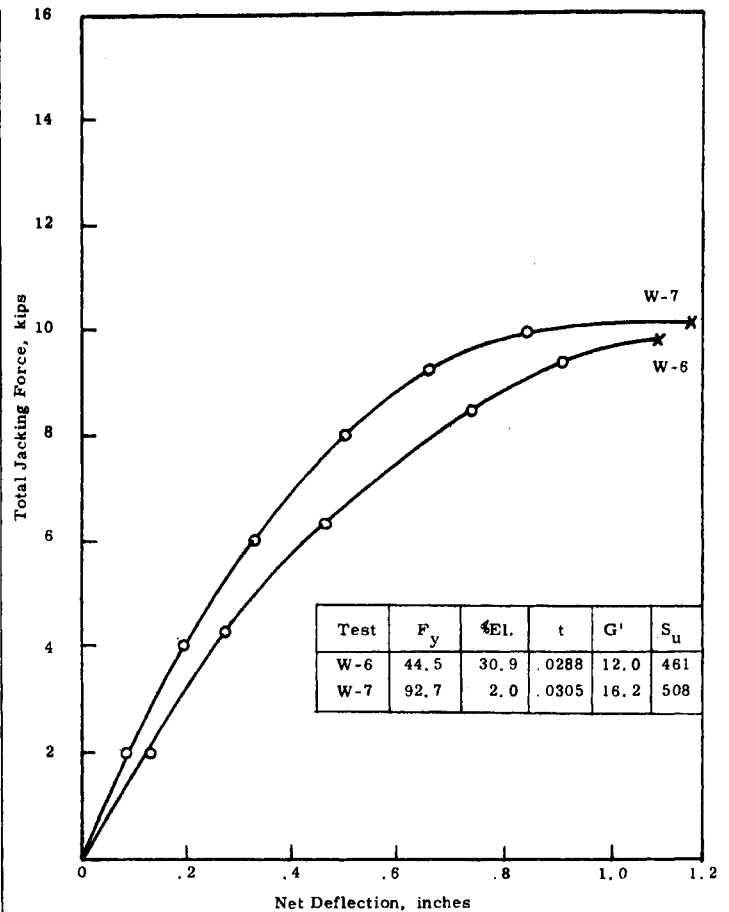


Fig. 16. Diaphragm Load-Deflection Curves Showing Influence of Material Yield Strength

type. Values of Q and M are shown below.

	A	I,W	WB
18 gage	\sqrt{n}	\sqrt{n}	n
20 gage	\sqrt{n}	\sqrt{n}	\sqrt{n}
22 gage	1	1	1

Where n = the number of welds per foot in the transverse direction.

Calculated values of stiffness can be increased by a coefficient M, depending on gage and panel type, as follows:

	A	I,W	WB
18 gage	\sqrt{n}	\sqrt{n}	\sqrt{n}
20 gage	\sqrt{n}	n	n
22 gage	\sqrt{n}	n	n

An extra weld has a greater effect on ultimate strength for the heavier gage diaphragms. In lighter gages, buckling failure predominates and an extra end weld has little effect on strength. It does, however, affect stiffness to a greater degree in the lighter gage diaphragms than in the heavier gages.

Purlin Spacing. Reduction of purlin spacing reduces the possibility of out-of-plane buckling and also increases the number of welds at any side lap, since panel to panel connections are made only at the purlins. In all cases, ultimate strength and stiffness are increased by a reduction in purlin spacing. The effect is more pronounced in the lighter gages, or those diaphragms which fail by strut-like buckling of a flute along

one edge of a panel.

Deck Profile. A flat sheet of light gage steel has almost no resistance to transverse bending, but may be highly resistant to in-plane shearing forces, assuming proper boundary conditions. When the same flat sheet is formed into a fluted shape, its transverse bending strength is increased tremendously, but its usefulness as a shear diaphragm is diminished. This comes about because a large percentage of the area of the plane in which the shear load is being applied, and hence the effective width over which shear must be transferred, is increased. The number and location of fasteners are now limited as well. Shear loads produce warping or distortion of the panel profile near the ends of the diaphragm, affecting both strength and stiffness. An example of panel end warping can be seen in Figure 17.

Narrow rib deck, which is conventionally assembled with its wide flat portion upward, has a very small part of its material in the shear plane and consequently is less stiff than intermediate or wide rib deck. If the strength and stiffness of narrow rib deck are taken as 1.0, then the other deck shapes tested can be assigned proportional coefficients as follows:

Deck Type	Strength	Stiffness
A	1.0	1.0
I	1.0	1.1
B	W	1.1
	WB	1.2

Deck profile appears to have a greater influence on stiffness than strength.

Side Lap Fasteners. Both diaphragm strength and stiffness may be increased as much as 25% by the addition of one intermediate side lap fastener mid-way between purlins. Since this connection is made between the two sheets and is not attached to the frame, it is difficult to make a good weld. Therefore, this fastener transfers very little shear, but even a poor weld can serve to change the buckling mode. Use of two or more side lap fasteners between purlins does not greatly improve the performance of the diaphragm and does not appear to justify the added labor cost.



Fig. 17. Warping of Steel Deck at Ends

MATHEMATICAL SOLUTION

The observation was made in the testing program that buckling, in some form, was present in all tests, whether or not it was the primary mode of failure. It was further noted that diaphragm behavior was sensitive to changes in span, i.e., purlin spacing, L , and thickness, t . This suggested the possibility of treating one flute of a deck panel as a column and solving for the buckling load in terms of some parameter such as L/t . Buckling was always observed to occur along a panel edge and was most severe on the first panel of the diaphragm, as illustrated in Figures 13, 14, and 15. This problem is complicated by the fact that a single flute is partially restrained by adjacent flutes and the load is applied eccentrically. If the restraining influence of the rest of the panel can be represented by three elastic springs, as shown in Figure 12, three equations of equilibrium can be written:

$$EI_y u'''' + Pu'' + Pa_y \phi'' + k_x (u + \bar{y}\phi) = 0 \quad (1)$$

$$EI_x v'''' + Pv'' - Pa_x \phi'' + k_y (v - \bar{x}\phi) = 0 \quad (2)$$

$$C_1 \phi'''' - (C - Pr_0^2) \phi'' + Pa_y u'' - Pa_x v'' + k_x (\bar{y}u + \bar{y}^2 \phi) + k_y (\bar{x}^2 \phi - \bar{x}v) + k_\phi \phi = 0 \quad (3)$$

If the spring constants k_x , k_y , and k_ϕ are allowed to go to zero, the problem is identical to the eccentrically loaded thin-walled column as solved by Pekoz and Winter (2). On the other hand, if the load is applied at the centroid, it becomes a problem of an elastically restrained column similar to that solved by Timoshenko and Gere (3).

Displacement functions were chosen to satisfy the end conditions due to the eccentric load as follows:

$$u = \frac{Pe_x}{2EI_y} (z^2 - Lz) + u_0 \sin \pi z/L \quad (4)$$

$$v = \frac{Pe_y}{2EI_x} (z^2 - Lz) + v_0 \sin \pi z/L \quad (5)$$

$$\phi = \phi_0 \sin \pi z/L \quad (6)$$

where u_0 , v_0 , and ϕ_0 are maximum displacements

The spring constant k_x , representing the restraint in a horizontal plane afforded by the adjacent flutes, will be quite large in relation to k_y or k_ϕ . Therefore, u_0 will be very small with respect to v_0 and ϕ_0 . If u_0 is considered negligible and Equations (5) and (6) are substituted into Equations (2) and (3), which are then rearranged into matrix form,

$$\begin{vmatrix} (P_{xe} - P) + k_y \frac{L^2}{\pi^2} & Pa_x + k_y \bar{x} \frac{L^2}{\pi^2} \\ Pa_x + k_y \bar{x} \frac{L^2}{\pi^2} & r_0^2 (P_{\phi e} - P) + \frac{FL^2}{\pi^2} \end{vmatrix} \begin{vmatrix} v_0 \\ \phi_0 \end{vmatrix} =$$

$$\begin{vmatrix} -4P^2 e_y \\ \pi P_{xe} \end{vmatrix} \quad (7)$$

$$\begin{vmatrix} 4P^2 a_x e \\ \pi P_{xe} \end{vmatrix} \quad (8)$$

That this is not a pure buckling problem is evident from the non-zero terms on the right side of the above equations. The flute will experience a certain amount of deflection prior to buckling, as was stated earlier. However, this precritical deflection is usually small, and so a homogeneous solution to the above equations should provide the desired information. It should be emphasized here that the mathematical solution was never intended to be able to predict the diaphragm ultimate strength. It was desired to determine whether a qualitative curve could

be developed which approximately matched the test results. The difficulty of trying to relate the actual buckling load on the model "column" to the shear load on the entire diaphragm is dramatized in Figure 18. At low load, the force on the welds along the edge may be assumed to be uniform. With increasing load, a tension field develops from A toward C with attendant warping and the force distribution on the welds may look more like that of Figure 18(b). The metal around the most heavily loaded welds will undergo deformation in the direction of the tension field. At weld number 4, there is no diagonal component to transmit the load to the support. With weld number 3 displaced toward number 4, the flute between is put into eccentric compression, causing it to bend upward. Increasing load causes increasing upward deflection until the flute buckles, either locally or wholly, as in Figures 14 and 15. This point is usually the ultimate load, even though minor increases in load were observed in some diaphragms beyond this point. The mathematical solution, then, only defines the buckling load on a flute between purlins; it has no means of relating this to the overall ultimate load on the diaphragm.

Solving the homogeneous solution, the buckling load is found to be the smallest load that will make the determinant vanish. Cross multiplying the determinant produces an equation of the form,

$$A P^2 + B P + C = 0 \quad (9)$$

Douty (4) makes the observation that A is insignificant for all but very short columns. Neglecting A and solving for P,

$$P = -\frac{C}{B} \quad (10)$$

or

$$P_{cr} = \frac{\frac{\pi^2}{L^2} (P_{xe} + k_y \frac{L^2}{\pi^2}) (C_1 K_{33} + \frac{CL^2}{\pi^2} + \frac{FL^4}{\pi^4}) - k_y^2 \bar{\alpha}^2 \frac{L^4}{\pi^4}}{\frac{\pi^2}{L^2} (P_{xe} + k_y \frac{L^2}{\pi^2}) + \frac{\pi^2}{L^2} (C_1 K_{33} + \frac{CL^2}{\pi^2} + \frac{FL^4}{\pi^4}) + 2a_x k_x \bar{\alpha} \frac{L^2}{\pi^2}} \quad (11)$$

Every variable in the right side of Equation (11) can be expressed as a function of L, the purlin spacing, and t, the sheet thickness. Substituting typical section properties for narrow, intermediate, and wide rib deck in terms of t and L into Equation (11), neglecting C, the torsional constant which is seen to be insignificant, collecting terms and performing the indicated division produces an infinite series. By substituting some typical values of t and L into the series, it can be determined that all terms beyond the third can be neglected. The resulting equations are the critical buckling loads for the three types of deck tested in this report:

Wide Rib:

$$P_{cr} = 68,700t/L^2 + 6.6t^3L^2 - 2.84 \times 10^{-5}t^5L^6 \quad (12)$$

Narrow Rib:

$$P_{cr} = 87,000t/L^2 + 4.0t^3L^2 - 1.60 \times 10^{-5}t^5L^6 \quad (13)$$

Intermediate Rib:

$$P_{cr} = 90,600t/L^2 + 5.27t^3L^2 - 1.837 \times 10^{-5}t^5L^6 \quad (14)$$

The mathematical solution is based on an over-simplified half-sine wave buckled shape, whereas test observations indicate that the deflected configuration more closely approximates that of a fixed-pinned column. This is clearly illustrated in Figure 15. If an effective length of 0.7L is substituted for L in Equations (12) through (14), the third term of the series becomes small in relation to the others and can be eliminated. The formulas then reduce to:

Wide Rib:

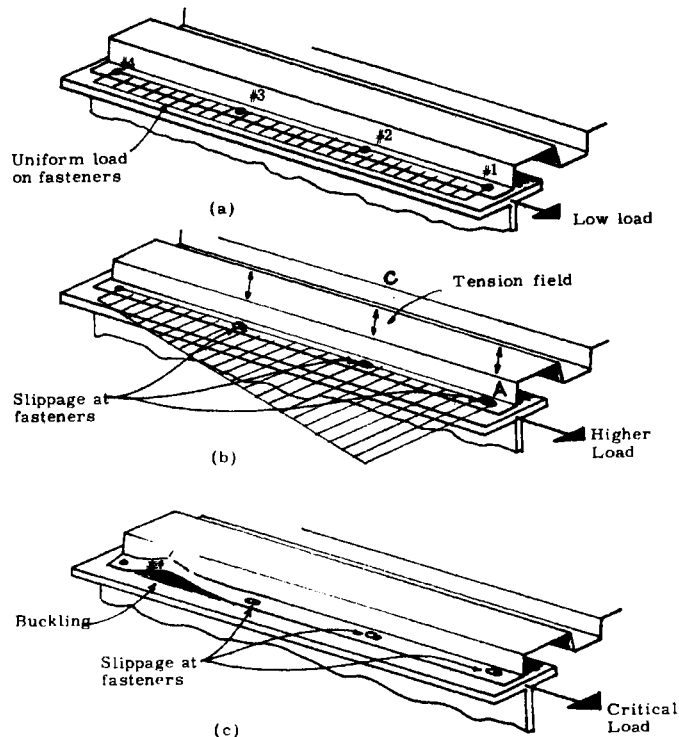


Fig. 18. Load Transfer on Edge Welds Prior to Buckling

$$P_{cr} = \frac{140,000}{L^2/t} + 3.3 t^3L^2 \quad (15)$$

Narrow Rib:

$$P_{cr} = \frac{174,000}{L^2/t} + 2.0 t^3L^2 \quad (16)$$

Intermediate Rib:

$$P_{cr} = \frac{180,000}{L^2/t} + 2.7 t^3L^2 \quad (17)$$

The first terms in Equations (15) through (17) represent the elastic buckling case, while the second terms show the restraining effect of the springs. They are identical in form to the solution for a centrally loaded column on an elastic foundation:

$$P_{cr} = \frac{EI \pi^2}{L^2} + k_y \frac{L^2}{\pi^2} \quad (18)$$

DESIGN CURVES

Substituting any given thickness t into Equations (15) through (17) and plotting P_{cr} against L/t produces a family of curves as shown in Figure 19. A failure envelope is obtained by constructing a curve tangent to the family of curves for specific thicknesses. Test results plotted on the same chart indicate that the shape of the theoretical curve is suitable even though the location is not. The latter is true because the load required to produce failure in the model column, represented by the left-hand ordinate of Figure 19, is some fraction of the total diaphragm load, represented by the right-hand ordinate.

If the magnitude of the failure envelope is adjusted to agree with total diaphragm failure load, and the equation is re-written in terms of L/t, it is seen in Figure 20 that all tests of the same thickness define straight lines which are approximately tangent to the theoretical failure envelope. If welds were adequate, all diaphragms would fail by

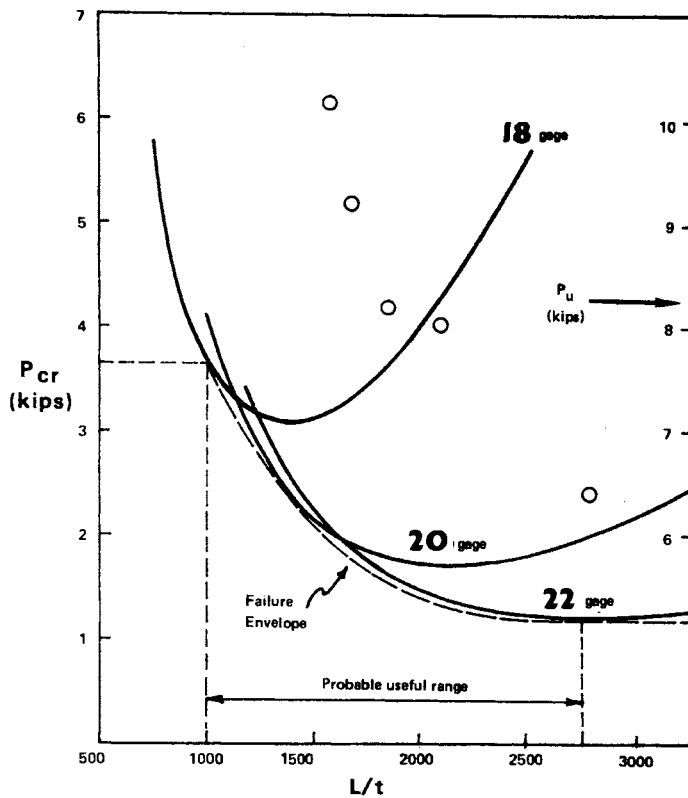


Fig. 19. Theoretical Solution to Diaphragm Buckling

buckling. Ideally though, when L/t is small, failure will usually occur in the welds. The curve in Figure 20 represents the pure buckling case and the straight lines show how strength is limited by weld failure before the buckling load can be reached. From this figure, a design chart can be constructed by dividing strength values by the AISI recommended safety factor of 2.4 and converting the diaphragm failure load, P_u , to the shear strength per foot, S_u , by dividing by the diaphragm length, b . The result is illustrated in Figure 21.

The shear strength of a steel deck-and-beam assembly may not be as important as stiffness in conventional construction. Consider a one-story rigid frame building with a flat roof of bar joists and steel deck as shown Figure 22. The deck is welded to the joists, rigid frames and eave members to form a shear-rigid diaphragm. When a wind load is applied to the side wall, the component of load at the center frame is resisted by both the rigid frame and the shear diaphragm. Each contributing resistance in proportion to its stiffness. Thus, in conventional steel deck installations, shear stiffness of the diaphragm is a more useful property for designers than ultimate strength, because of its interaction with other structural elements.

An attempt to relate diaphragm stiffness to the "stiffness" of the model column was unsuccessful because many of the factors that affect stiffness, such as end warping, were neglected in the mathematical solution. For this reason, the stiffness design charts have been developed empirically.

When experimental stiffness values are plotted against $L/t \cdot a/b$, all tests of like thickness are seen to describe reasonably straight lines, with the heaviest gages having the steepest slopes. (See Figure 23). It can also be observed that the straight line segments generally describe the same kind of curve as before, but the curve really has no

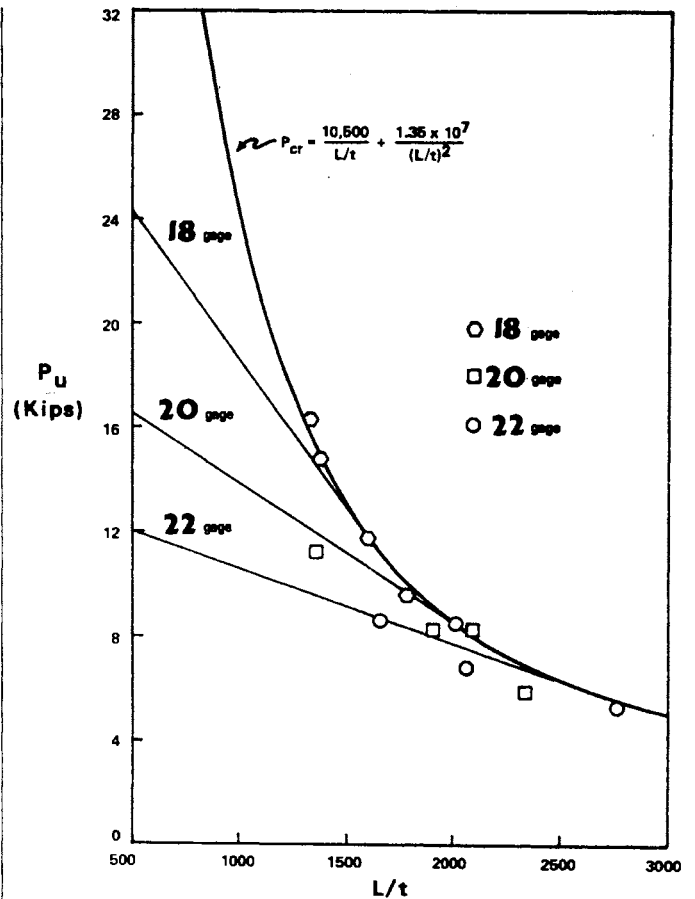


Fig. 20. Ultimate Shear Strength Curve

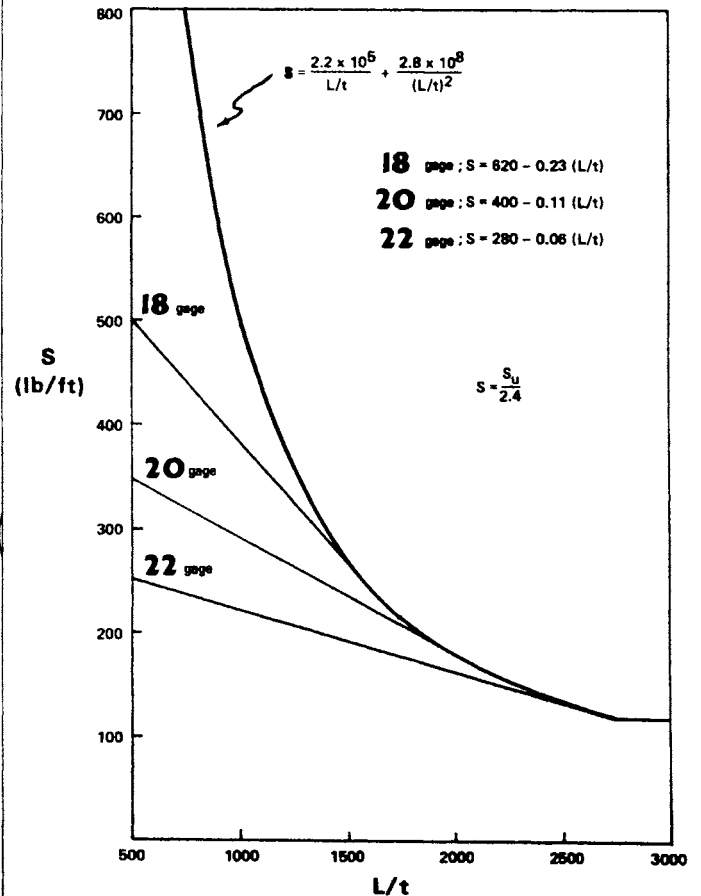


Fig. 21. Diaphragm Strength Curve

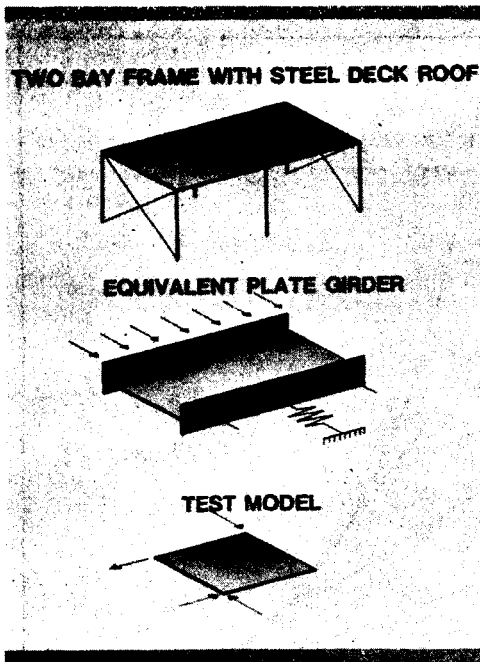


Fig. 22. Interaction of Roof Diaphragm with Structural Framework

significance, since it does not represent an upper limit. Therefore, a stiffness design chart, such as Figure 24, is better left in straight line form with reasonable limits defined on either end. To put the abscissa of Figure 24 in proper perspective, the upper limit of 3000 on 20 gage deck corresponds to a square diaphragm with purlins spaced on 9'-0 centers. The lower limit corresponds to the same diaphragm with 3'-0 purlin spacing.

Charts such as those of Figures 21 and 24 have been developed for

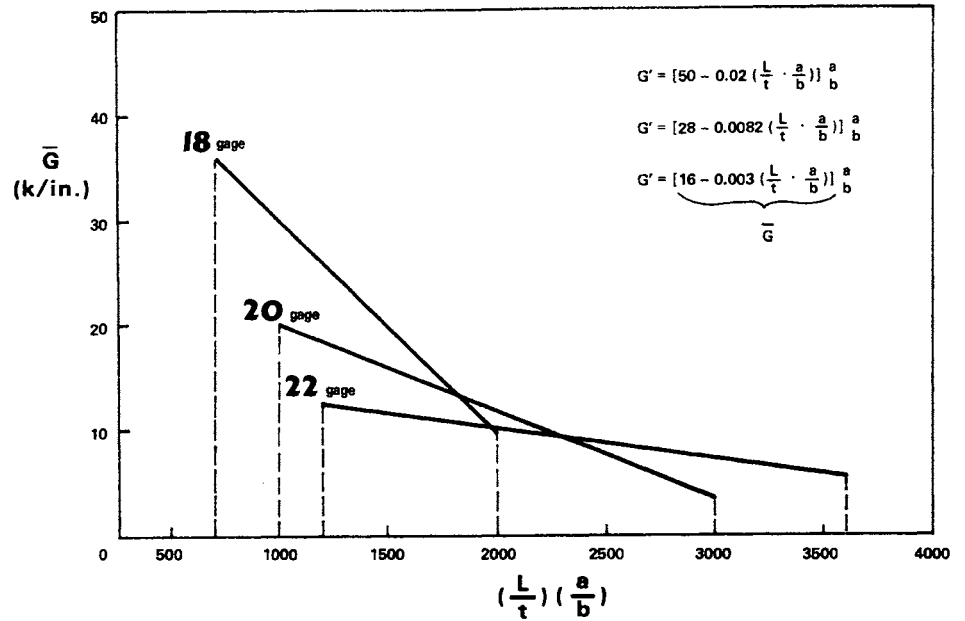


Fig. 24. Stiffness Design Curve

all three types of deck tested in this investigation, and formulas have been derived from the curves. These recommended design formulas are summarized in Tables 2 and 3. In addition, modification factors are given in the tables for conditions which are not standard, such as a different weld arrangement, and non-standard width panels. These modifiers, whose product should not exceed 2.0, were suggested by the comparison of load-deflection curves of nearly-similar tests as described earlier in this report.

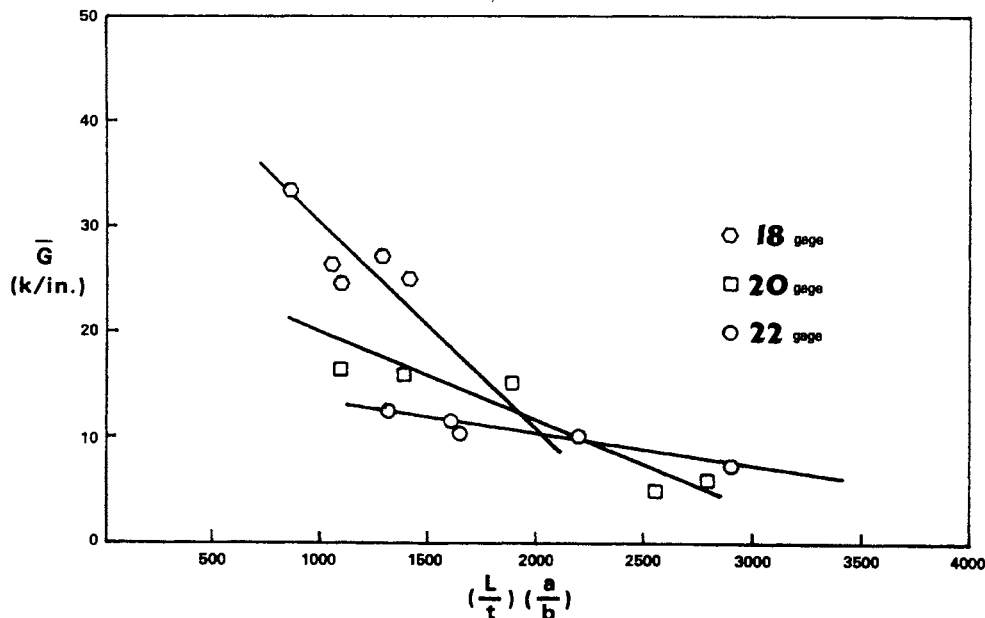


Fig. 23. Experimental Stiffness vs. $(L/t \cdot a/b)$

Table 2. Summary of design formulas for steel deck diaphragm strength
(a) 24" wide panel *12*12* weld spacing, no intermediate side lap fasteners

Nom. Gage	Narrow Rib (A)	Intermediate Rib (I)	Wide Rib (W)	Wide Rib (WB)
(1) All	$S = \frac{2.2 \times 10^5}{L/t} + \frac{2.8 \times 10^8}{(L/t)^2}$		$S = \frac{2.88 \times 10^5}{L/t} + \frac{2.62 \times 10^8}{(L/t)^2}$	$S = \frac{2.5 \times 10^5}{L/t} + \frac{3.75 \times 10^8}{(L/t)^2}$
(2)	18	$S = 620 - 0.23(L/t)$	$S = 700 - 0.26(L/t)$	Use formula (1)
	20	$S = 400 - 0.11(L/t)$	$S = 400 - 0.10(L/t)$	$S = 480 - 0.13(L/t)$
	22	$S = 280 - 0.06(L/t)$	$S = 280 - 0.05(L/t)$	$S = 350 - 0.074(L/t)$

Note: Compute S by both formulas (1) and (2) and use the smaller value.

(b) Modification factors for above formulas for non-standard conditions

Nom. Gage	If an extra weld is added at the panel ends, multiply S by (n = no. welds/foot)			
18	$\sqrt[n]{n}$	$\sqrt[n]{n}$	$\sqrt[n]{n}$	n
20	$\sqrt[n]{n}$	$\sqrt[n]{n}$	$\sqrt[n]{n}$	$\sqrt[n]{n}$
22	1	1	1	1

If panel width is other than 24", multiply S by $\sqrt{w/24}$ for all cases, where w = panel width.
If intermediate side lap fasteners are present, multiply S by 1.25.
Product of all modification factors should not exceed 2.0.

Table 3. Summary of design formulas for steel deck diaphragm stiffness
(a) 24" wide panel, *12*12* weld spacing, no intermediate side lap fasteners

Nom. Gage	Narrow Rib (A)	Intermediate Rib (I)	Wide Rib (W)	Wide Rib (WB)
18	$700 < \frac{L}{t} \cdot \frac{a}{b} < 2000$ $G' = \left[50 - 0.02 \left(\frac{La}{tb} \right) \right] \frac{a}{b}$		$700 < \frac{L}{t} \cdot \frac{a}{b} < 1600$ $G' = \left[75 - 0.04 \left(\frac{La}{tb} \right) \right] \frac{a}{b}$	
20	$1000 < \frac{La}{tb} < 3000$ $G' = \left[27 - 0.0075 \left(\frac{La}{tb} \right) \right] \frac{a}{b}$		$1000 < \frac{La}{tb} < 3000$ $G' = \left[30 - 0.0085 \left(\frac{La}{tb} \right) \right] \frac{a}{b}$	
22	$1200 < \frac{L}{t} \cdot \frac{a}{b} < 3600$ $G' = \left[16 - 0.003 \left(\frac{La}{tb} \right) \right] \frac{a}{b}$	$1200 < \frac{L}{t} \cdot \frac{a}{b} < 3600$ $G' = \left[22 - 0.0045 \left(\frac{La}{tb} \right) \right] \frac{a}{b}$		

(b) Modification factors for above formulas for non-standard conditions

Nom. Gage	If an extra weld is added at the panel ends, multiply S by: (n = no. welds/foot)			
18	$\sqrt[n]{n}$	$\sqrt[n]{n}$	$\sqrt[n]{n}$	$\sqrt[n]{n}$
20	$\sqrt[n]{n}$	n	n	n
22	$\sqrt[n]{n}$	n	n	n

If panel width is other than 24", multiply G' by $\sqrt{w/24}$ for all cases, where w = panel width.
If intermediate side lap fasteners are present, multiply G' by 1.25.
Product of all modification factors should not exceed 2.0.

CONCLUSIONS

The major variables affecting shear diaphragm behavior are the material thickness, t, and the purlin spacing, L. From tests, it was observed that diaphragms fail by tearing around the welds, by strut-like buckling of an edge flute between purlins, or some combination of the two. As a means of predicting in advance the performance of any given steel deck shear diaphragm, a mathematical model was formulated based on the stability of a single corrugation or flute. The flute column was eccentrically loaded and the effects of adjacent flutes simulated by elastic springs. The solution to the model worked well for predicting ultimate strength, even though there were some problems in trying to relate the critical buckling load on a single flute to the

total shear load on the diaphragm. More difficulty was encountered in attempting to derive a formula for stiffness from the same model. Stiffness was found to be influenced by too many factors which were neglected in the mathematical solution, such as overall diaphragm length. Stiffness is also extremely sensitive to shear deflection which is a combination of in-plane shear strains, deformation of the material around welds, panel end warping, and slip in the frame connections. None of these were accounted for in the theoretical development of the stiffness formulas.

The results of this investigation indicate that the method of relating diaphragm behavior to the stability of one flute between purlins predicts ultimate strength reasonably well, but is not adequate for predicting stiffness.

EXAMPLE

Determine the allowable design strength and shear stiffness of a diaphragm which is 21' square and is made of 18 gage, 24" wide rib deck, W type, with purlins on 3'-6" centers and standard welds.

$$\frac{L}{t} = \frac{42}{0.0478} = 880$$

From Table 2,

$$(1) S = \frac{2.88 \times 10^5}{880} + \frac{2.62 \times 10^8}{(880)^2}$$

$$S = 327 + 338 = 665 \text{ lb/ft.}$$

$$(2) S = 700 - 0.26(880)$$

$$S = 700 - 229 = 471 \text{ lb/ft.}$$

Formula (2) controls, $\therefore S = 471 \text{ lb/ft.}$

$$\left(\frac{L}{t}\right) \left(\frac{a}{b}\right) = 880 \cdot \frac{21'}{21'} = 880$$

From Table 3,

$$G' = [50 - 0.02(880)] \frac{21}{21} = 32.4 \text{ k/in.}$$

REFERENCES

- American Iron and Steel Institute, Design of Light Gage Steel Diaphragms, 1967.
- Pekoz, T. B., and G. Winter, "Torsional-Flexural Buckling of Thin-Walled Sections Under Eccentric Load," Journal of the Structural Division, ASCE, Vol. 95, No. ST5, May, 1969.
- Timoshenko, S. P., and J. Gere, "Theory of Elastic Stability," McGraw-Hill.
- Douty, R. T., "A Design Approach to the Strength of Laterally Unbraced Compression Flanges," Cornell University Engineering Experiment Station Bulletin No. 37, April, 1962.

LIST OF SYMBOLS

- a Total width of diaphragm measured perpendicular to flutes (ft).
- a_x Horizontal distance from shear center of deck flute to point of load application (in).
- a_y Vertical distance from shear center of deck flute to point of application (in).
- A Cross-sectional area of single deck flute (in^2).
- b Total length of diaphragm, measured parallel to flutes (ft).
- c Centroid of deck flute.
- C Torsional rigidity of single deck flute = GK (kip-in²).
- C_1 Warping rigidity of single deck flute = EC_w (kip-in⁴).
- C_w Warping constant of single flute (in⁶).

- d Nominal depth of steel deck (in).
- e_x, e_y Eccentricities of loading with respect to centroid of deck flute (in).
- E Modulus of elasticity of steel (29,500,000 psi).
- F $k_x \bar{y}^2 + k_y \bar{x}^2 + k_\phi$ (lb)
- G Shear modulus for steel (11,500,000 psi).
- \bar{G} Slope of tangent to load-deflection curve at $0.4 P_U$ (kips/in).
- G' Shear stiffness of diaphragm (kips/in) $\bar{G} \cdot a/b$.
- h Nominal width of maximum flat portion of deck flute (in).
- h_x, h_y Coordinates of elastic support axis, N, relative to centroid of deck flute (in).
- I_x, I_y Moments of inertia of single flute about its x and y axes, respectively (in⁴).
- I_o Polar moment of inertia of a single flute about its shear center (in⁴).
- k_x, k_y, k_ϕ Elastic spring constants applied to single deck flute in direction of x and y axes and around z axis.
- K Torsional constant of deck flute (in⁴).
- L Distance between purlins in diaphragms tests (in).
- M Modification factors for stiffness design formulas.
- n Number of welds per foot of diaphragm width.
- P_{xe}, P_{ye} Elastic axial buckling loads of deck flute column about x and y axes, respectively (kips).
- $P_{\phi e}$ Torsional buckling load of deck flute column about longitudinal axis (lips).
- P_{cr} Critical load on deck flute column.
- P_u Ultimate shear load on diaphragm.
- Q Modification factors for strength design formulas.
- t Uncoated thickness of steel deck (in).
- u Deflection component of deck flute in direction of x axis.
- v Deflection component of deck flute in direction of y axis.
- u_o, v_o, ϕ_o Maximum homogeneous displacements in x and y directions and about z axis.
- w Width of steel deck panel (in).
- x, y, z Principal axes of flute for mathematical solution.
- \bar{x} $x_o - h_x$ (in).
- \bar{y} $y_o - h_y$ (in).
- x_o Horizontal distance between centroid and shear center of single deck flute (in).
- y_o Vertical distance between centroid and shear center of single deck flute (in).
- α Coefficient relating change in thickness to changes in stiffness and strength.
- ϕ Angle of twist of deck flute about the z axis.
- β_1 $1/I_x \left[\int_A y^3 dA + \int_A x^2 y dA \right] - 2y_o$
- β_2 $1/I_y \left[\int_A x^3 dA + \int_A y^2 x dA \right] - 2x_o$
- Δ Shear deflection of diaphragm.